REEL-C 6492

A.T.I 162246

UNCLASSIFIED

ATI 162 246 (Copies obtainable from ASTIA-DSC)

Massachusetts Institute of Technology, Aero-Elastic and Structures Research, Cambridge

A Note on Large Plastic Deformations of Beams Under Transverse Impact - and Appendix A - Technical Report

Pian, T.H.H. 14 May'52 40pp. diagrs, graphs

USN Contr. No. N5ori-07833

Beams - Stress analysis
Deformation, Plastic

Aircraft Structures (7)
Theory (2)

UNCLASSIFIED

MASSACHUSETTS INSTITUTE OF TECHNOLOGY
Department of Aeronautical Engineering

CONTRACT NO. N5ori-07833
NR-064-259

72

A NOTE

ON

LARGE PLASTIC DEFORMATIONS OF BEAMS UNDER TRANSVERSE IMPACT

TECHNICAL REPORT

ON

CONTRACT N5ori-07833

FOR

OFFICE OF NAVAL RESEARCH

BY THE

MASSACHUSETTS INSTITUTE OF TECHNOLOGY

MAY 14, 1952

Reported by: T. H. H. Pian
T. H. H. Pian

Approved by: R. L. Bisplinghoff
R. L. Bisplinghoff

AERO-ELASTIC AND STRUCTURES RESEARCH

ACKNOWLEDGEMENT

The author wishes to express his gratitude to Prof. R. L. Bisplinghoff for his guidance to the research program.

Thanks are due to Mr. G. Isakson for his suggestions.

Computing was performed under the supervision of Miss. Winifred Dunlop.

Typing was done by Miss. Eleanor Mugnai, and illustrations were prepared by Miss. Marilyn A. Squires.

TABLE OF CONTENTS

Summary

The method of Lee and Symonds (Brown University Report B11-3/28, ONR Contract N7onr-35810, NR-360-364) of analyzing plastic deformations of beams under transverse impact is adopted to determine the plastic strains in a simply supported uniform beam subjected to a concentrated impulsive load at the center of the beam. The "plastic-rigid" theory is used.

It is shown that in the case of a simple square-shape impulsive load, the problem, which involves a non-linear differential equation, can be solved in closed form. The time histories of the acceleration, the velocity, and hence, the displacement are then evaluated. Results are presented in terms of the permanent deformation caused by the impact.

I Introduction

In a recent report (Ref. 1) Lee and Symonds have developed a method of calculating the permanent deformations of beams of ductile material subjected to transverse impact loadings. The analysis in Reference 1 is based on the "plastic-rigid" assumption such that the moment-curvature relation is of the type shown in Figure 1. In this figure M_0 is the limiting bending moment for which the plastic regions spread over the whole cross-

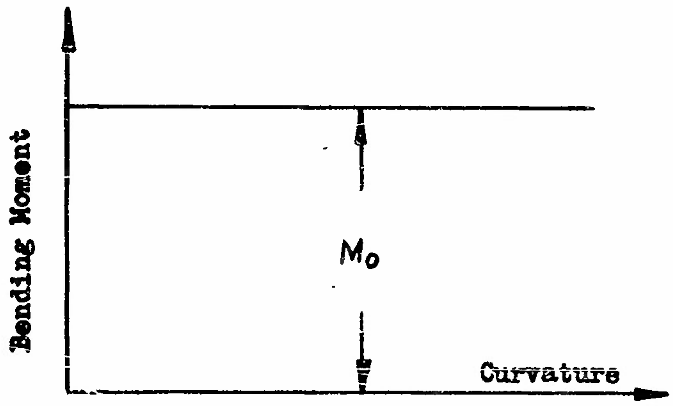

Figure 1. Moment-Curvature of a "Plastic-rigid" beam.

section of the beam. The analysis also assumes that the beam has an infinite rigidity at any section until the limit moment M_0 is reached. When this limit is reached a plastic hinge is formed and the beam bends in the form of a sharp kink.

The introduction of the idealized "plastic-rigid" assumption eliminates the consideration of elastic vibrations of the beam, and hence simplifies the analysis greatly. It is expected that this type of analysis is only applicable to cases in which the plastic strains are large compared with elastic strains. Lee and Symonds have presented a criterion regarding the limitation of their method.

In Reference 1 the problem of a force in the form of a triangular pulse applied at the mid-point of a uniform beam with free ends has been analyzed. It has been shown that under small load, the beam performs a rigid-body translation motion; under moderate load, a plastic hinge is formed at the mid-span of the beam; while at very high load, two additional plastic hinges are formed, one on each side of the mid-span hinge. The hinge point on either side has been shown to move toward the center as the load increases, while away from the center as the load decreases. The calculation of this phase of the motion involves the solution of a non-linear differential equation. In general, methods of successive approximation, or of step-by-step integration, must be employed.

The present report is an application of the assumptions and the method of Reference 1 to the determination of plastic strains in a simply supported uniform beam subjected to a concentrated impulsive load at the center of the beam. Dynamical equations comparable with those of Reference 1 are obtained. It will be shown, however, that when the impulsive load is of a square-shape, the solutions are simplified. In fact, the non-linear differential equation can be solved in closed form, and the time histories of the acceleration, the velocity and the displacement of the beam can be easily evaluated.

II Dynamical Equations

We shall consider a simply supported uniform beam subjected to a concentrated impulsive load P(t) at the center of the span, as shown in Figure 2. The load P(t) is assumed to increase from zero to a maximum value,

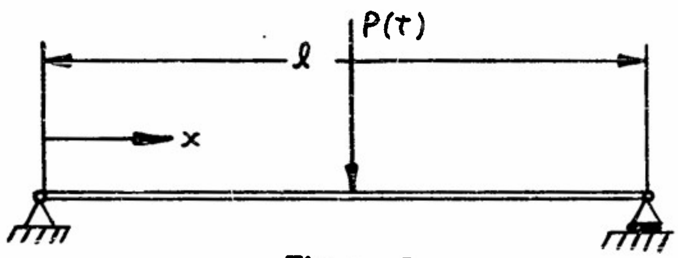

Figure 2.

and then decrease to zero. The beam is assumed to be straight and rigid at the initial instant.

In the first phase of the impact when no plastic deformation occurs, the beam remains rigid. The bending moment distribution is given by

$$\begin{aligned} M(x) &= P x/2 \qquad \text{for } 0 < x < \ell/2 \\ &= P(\ell - x)/2 \qquad \text{for } \ell/2 < x < \ell \end{aligned} \tag{1}$$

where x is measured from one end of the beam. The loading, shear, and moment diagrams are shown in Figure 3. The maximum bending moment, of course, occurs at the middle of the beam and is equal to

$$M(\ell/2) = P\ell/4 \tag{2}$$

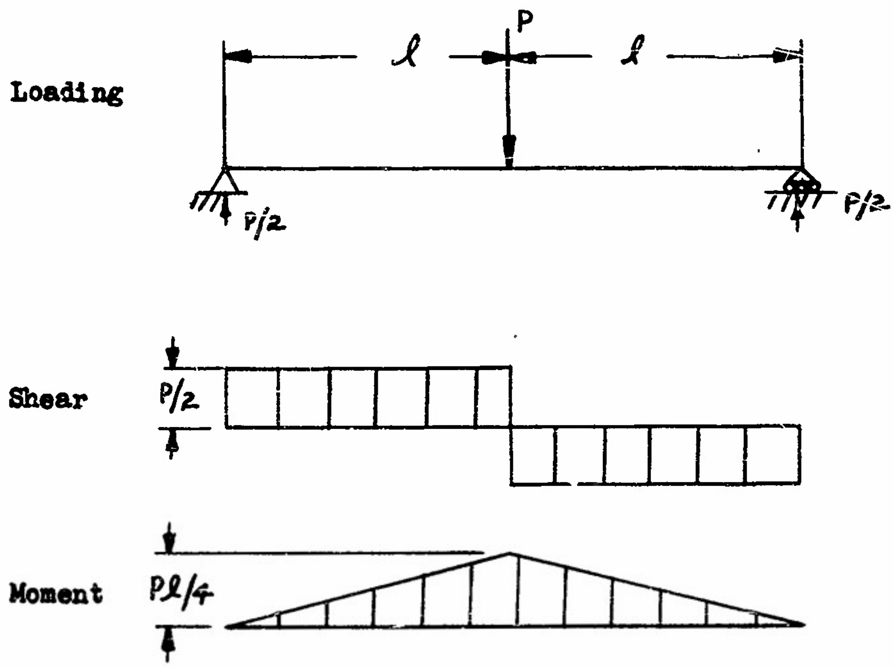

Figure 3.

This first phase of motion ends when the moment at the mid-span reaches M_0, and a plastic-hinge is formed. We shall introduce a symbol μ for the non-dimensional parameter $P\ell/M_0$. Thus the beam remains stationary when $\mu < 4$.

In the second phase of motion when $\mu > 4$, the beam may be analyzed by placing a plastic hinge at the center. The two halves of the beam remain rigid but rotate with respect to each other as shown in Figure 4(a).

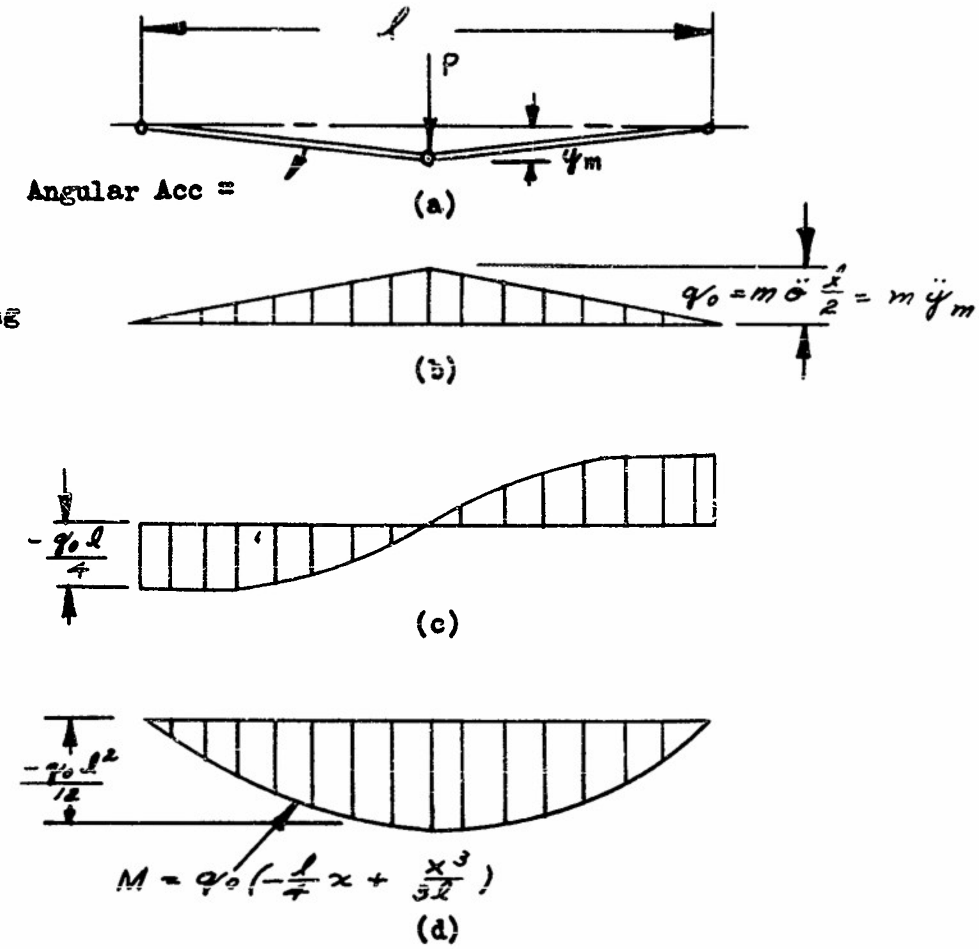

Figure 4.

The acceleration of the beam is to be determined by the condition that, at the center of the span, the resulting moment due to both the applied load and the inertia load should be equal to the limiting moment M_o. The inertia loading, shear and moment diagrams are shown respectively in Figure 4(b) (c) and (d). The maximum inertia loading is denoted by the symbol g_o. The distribution of bending moment corresponding to the inertia loading is thus,

$$M = q_o\left(-\frac{l}{4}x + \frac{x^3}{3l}\right) \tag{3}$$

and the bending moment at the mid-span is $-q_o l^2/12$.

The total bending moment can be obtained by combining equations (1) and (3)

$$M = \frac{Px}{2} - q_o\left[\frac{lx}{4} - \frac{x^3}{3l}\right] \tag{4}$$

The moment at mid-span is $\left(\frac{Pl}{4} - \frac{q_o l^2}{12}\right)$. By setting this equal to M_o and solving for g_o we obtain

$$q_o = \frac{3M_o}{l^2}(\mu - 4) \tag{5}$$

The linear acceleration at the mid-span is thus,

$$\ddot{y}_m = \frac{q_o}{m} = \frac{3M_o}{ml^2}(\mu - 4) \tag{6}$$

It should be remembered that this equation applies only after μ has reached the value 4, since the beam is stationary up to this point. The linear velocity and displacement at the mid-span can be evaluated by integration of Equation (6).

The second phase of motion ends when the bending moment at another point along the beam reaches the limiting value M_o. By substituting Equation (5) into (4) and by introducing the symbol ξ to replace the non-dimensional parameter x/ℓ, we obtain,

$$M(\xi) = M_0\left[\mu\left(\xi^3 - \frac{1}{4}\xi\right) + 3\xi - 4\xi^3\right] \tag{7}$$

The maximum bending moment occurs at the point where $dM/d\xi = 0$, or

$$3(\mu - 4)\xi^2 = \frac{1}{4}\mu - 3$$

or

$$\xi = \sqrt{\frac{\mu - 12}{12(\mu - 4)}} \tag{8}$$

Substituting this value into Equation (7), we obtain the expression of the maximum bending moment in terms of the loading parameter μ. By setting this expression equal to the limiting bending moment $-M_0$, we obtain the value of μ at which the second plastic hinge is formed. We obtain the following equation for μ,

$$(\mu - 12)^{3/2} = 12\sqrt{3}(\mu - 4)^{\frac{1}{2}} \tag{9}$$

The only real root of this equation is

$$\mu = 36 \tag{10}$$

The corresponding value of ξ is, from Equation (8),

$$\xi = 1/4 \tag{11}$$

Thus, the second plastic hinge is located at the quarter span point.

The third phase of motion commences when the load is further increased so that $\mu > 36$. It can be seen, by a similar argument given in Reference 1, that the equilibrium conditions in this phase of motion can be satisfied only when the hinge point on either side of the mid-span hinge moves as the load increases. As soon as the hinge has moved to a new position the bending moment at the previous hinge location must drop to a value smaller than M_o, and no further rotation occurs there. Thus the segments to the right and left of this moving hinge move as rigid bodies. Also at each section where the instantaneous hinge is located, the relative rotation is infinitesimal and the slope angle changes continuously through the segment through which the hinge has passed. This is shown in Figure 5.

We define the motion of the beam by the slope θ_0 and θ_1, the angular velocities $\dot{\theta}_0$ and $\dot{\theta}_1$, and the angular accelerations $\ddot{\theta}_0$ and $\ddot{\theta}_1$, of the two rigid segments, and denote the location of the hinge point by x_h as shown in Figure 5.

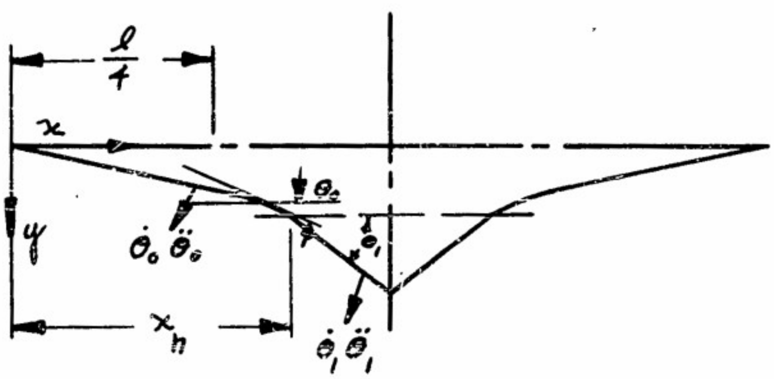

Figure 5.

We see that the displacement of the beam can be expressed by

$$y = \begin{cases} \int_0^x \theta_o \, dx & \text{for } x < x_h \\ \int_0^{x_h} \theta_o \, dx + \theta_1 (x - x_h) & \text{for } x > x_h \end{cases} \tag{12}$$

Thus, the velocity of the beam obtained by differentiating Equation (12), is

$$\dot{y} = \begin{cases} \dot{\theta}_o x & \text{for } x < x_h \\ \dot{\theta}_o x_h + \dot{\theta}_1 (x - x_h) + \dot{x}_h (\theta_1 - \theta_o) & \text{for } x_h < x < \ell/2 \end{cases} \tag{13}$$

since the slope of the beam is continuous at the travelling hinge, $(\theta_1 - \theta_o)$ vanishes, and Equation (13) can be rewritten as

$$\dot{y} = \begin{cases} \dot{\theta}_o x & \text{for } x < x_h \\ \dot{\theta}_o x_h + \dot{\theta}_1 (x - x_h) & \text{for } x_h < x < \ell/2 \end{cases} \tag{13a}$$

Similarly, the acceleration of the beam, can be expressed by

$$\ddot{y} = \begin{cases} \ddot{\theta}_o x & \text{for } x < x_h \\ \ddot{\theta}_o x_h + \ddot{\theta}_1 (x - x_h) - \dot{x}_h (\dot{\theta}_1 - \dot{\theta}_o) & \text{for } x_h < x < \ell/2 \end{cases} \tag{14a}$$

Equation (14a) can be rewritten as

$$\ddot{y} = \begin{cases} \ddot{\theta}_o x & \text{for } x < x_h \\ \ddot{\theta}_o x + (\ddot{\theta}_1 - \ddot{\theta}_o)(x - x_h) - \dot{x}_h (\dot{\theta}_1 - \dot{\theta}_o) & \text{for } x_h < x < \ell/2 \end{cases} \tag{14b}$$

It can be seen that the acceleration, and hence the inertia loading of the beam, can be divided into three components, as shown in Figure 6. We

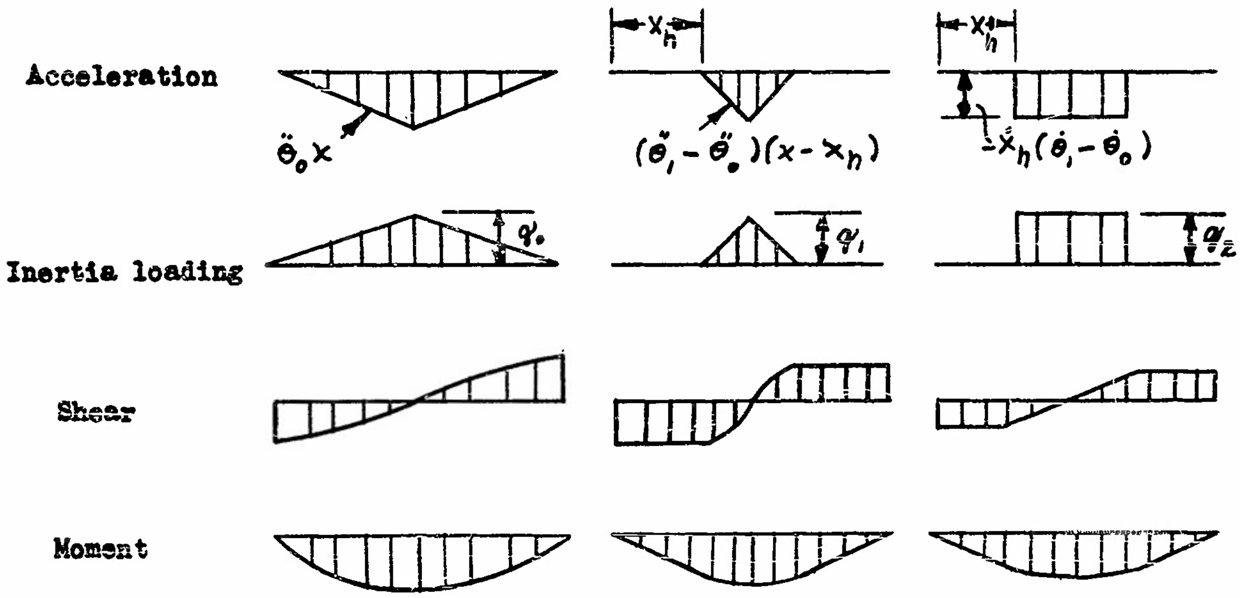

Figure 6.

shall designate these three components by their maximum values g_0, g_1, and g_2. The relations between these quantities and the acceleration of the beam are,

$$q_0 = \ddot{\theta}_0 \, l / 2m \tag{15}$$

$$q_1 = (\ddot{\theta}_1 - \ddot{\theta}_0)(l/2 - x_h)/m \tag{16}$$

$$q_2 = -\dot{x}_h(\dot{\theta}_1 - \dot{\theta}_0)/m \tag{17}$$

It can also be seen that the linear acceleration at the center of the beam is

$$\ddot{y} = (q_0 + q_1 + q_2)/m \tag{18}$$

The shear and moment distributions corresponding to these loadings are also shown in Figure (6). The bending moment due to g_0 is the same as that given in Equation (3). The moment due to g_1 and g_2 are respectively

$$M = \begin{cases} -q_1(\ell - 2x_h)x/4 & \text{for } x < x_h \\ \dfrac{q_1}{12(\ell - 2x_h)}\left[-4x_h^3 + 3(4x_h - \ell)\ell x - 12x_h x^2 + 4x^3\right] & \text{for } x > x_h \end{cases} \tag{19}$$

$$M = \begin{cases} -q_1(\ell - 2x_h)x/2 & \text{for } x < x_h \\ q_2(x_h^2 - \ell x + x^2)/2 & \text{for } x > x_h \end{cases} \tag{20}$$

The values of g_0, g_1 and g_2 are to be determined by the conditions that both at the center of the span and at the hinge point x_h, the resulting bending moment is equal to M_0, and that the bending moment at the hinge point x_h should be a maximum. Thus by summing up Equations (1) (3) (19) and (20), and setting $M_{x=\ell/2} = M_0$, $M_{x=x_h} = -M_0$ and $\left(\frac{dM}{dx}\right)_{x=x_h} = 0$, and by introducing the non-dimensional parameters μ and ξ_h $(= x_h/\ell)$, we obtain the following system of equations,

$$\begin{cases} \frac{1}{12} g_0 (3\xi_h - 4\xi_h^3) + \frac{1}{4} g_1 (1 - 2\xi_h)\xi_h + \frac{1}{2} g_2 (1-2\xi_h)\xi_h = (\frac{1}{2}\mu\xi_h + 1)\frac{M_0}{\ell^2} \\ \frac{1}{12} g_0 + \frac{1}{12} g_1 (1+\xi_h)(1-2\xi_h) + \frac{1}{8} g_2 (1-2\xi_h)(1+2\xi_h) = (\frac{1}{4}\mu - 1)\frac{M_0}{\ell^2} \\ \frac{1}{4} g_0 (1 - 4\xi_h^2) + \frac{1}{4} g_1 (1-2\xi_h) + \frac{1}{2} g_2 (1-2\xi_h) = \frac{1}{2}\mu\frac{M_0}{\ell^2} \end{cases} \tag{21}$$

These equations are sufficient to express the unknown quantities g_0, g_1 and g_2 in terms of the parameters μ and ξ_h. However in order to evaluate ξ_h a fourth equation is required. This equation arises from a relation between g_1 and g_2, given by Equations (16) and (17). We have, from Equations (16) and (17),

$$(\ddot{\theta}_1 - \ddot{\theta}_0) = m\, g_1 / \frac{\ell}{2} - x_h \tag{22}$$

$$(\dot{\theta}_1 - \dot{\theta}_0) = -m\, g_2 / x_h \tag{23}$$

and by observing that $(\ddot{\theta}_1 - \ddot{\theta}_0)$ is the derivate of $(\dot{\theta}_1 - \dot{\theta}_0)$ we can write,

$$g_1 / \frac{\ell}{2} - x_h = -\frac{d}{dt}(g_2 / x_h) \tag{24}$$

or in terms of non-dimensional parameters,

$$g_1 / 1 - 2\xi_h = -\frac{d}{dt}(g_2 / 2\xi_h) \tag{25}$$

From Equations (21) we obtain,

$$q_0 = \frac{3}{2} \frac{1}{\xi_h^3} \frac{M_0}{\ell^2} \tag{26}$$

$$q_1 = \frac{3}{2(1-2\xi_h)} \left(4\mu - \frac{1-6\xi_h+12\xi_h^2+56\xi_h^3}{(1-2\xi_h)\xi_h^3}\right) \frac{M_0}{\ell^2} \tag{27}$$

$$q_2 = \frac{2}{1-2\xi_h} \left(-\mu - \frac{3}{2} \frac{(1-4\xi_h-12\xi_h^2)}{(1-2\xi_h)\xi_h^2}\right) \frac{M_0}{\ell^2} \tag{28}$$

Substituting Equations (27) and (28) in (25), we obtain a non-linear differential equation, the solution of which gives the time history of the hinge position ξ_h. Having evaluated ξ_h we can calculate the time history of the inertia loadings, g_0, g_1 and g_2 by using Equations (26) (27) and (28).

The equations (25) to (28) are still applicable during the period when the applied force has reached its maximum value and starts to decrease. This phase of motion terminates, however, when the motion has been decelerating such that the relative angular velocity $(\dot{\theta}_1 - \dot{\theta}_0)$ has become zero, and hence, the plastic hinge at $x = x_h$ removed.

In the succeeding period, the beam will again move with its two halves remaining rigid but rotating against each other about a hinge point at the center. This final motion ends when the angular motion decreases to zero.

III Application to the Case of a Square Impulse

The solutions given in the proceeding section are now applied to the problem of a simply supported beam under a concentrated center load in the form of a square shape impulse of amplitude P_m, and period T, as shown in Figure 7. We shall discuss the problem in three parts according to the range

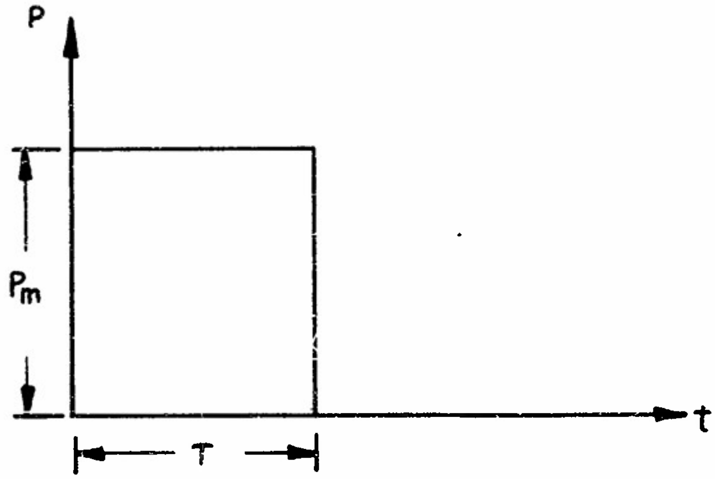

Figure 7.

of the amplitude of the load. We denote the non-dimensional parameter $P_m \ell / 4 M_o$ by the symbol μ_m.

(a) $\mu_m < 4$ In this case the beam remains undeformed.

(b) $4 < \mu_m < 36$ During the period $t < T$, when the loading is applied, the linear acceleration at the center of the beam is given by Equation (6), i.e.,

$$\ddot{y}_m = \frac{3 M_o}{m \ell^2} (\mu_m - 4) \qquad (29)$$

The linear velocity and linear displacement at this point, are respectively,

$$\dot{y}_m = \frac{3 M_o}{m \ell^2} (\mu_m - 4) t \tag{30}$$

and

$$y_m = \frac{3 M_o}{2 m \ell^2} (\mu_m - 4) t^2 \tag{31}$$

The maximum displacement, expressed in terms of non-dimensional parameters, is

$$y_m \Big/ \frac{M_o T^2}{m \ell^2} = \frac{3}{2} (\mu_m - 4) \left(\frac{t}{T}\right)^2 \tag{32}$$

For $t > T$, the acceleration at the center becomes

$$\ddot{y}_m \Big/ \frac{M_o}{m \ell^2} = -12 \tag{33}$$

and the velocity and displacement are,

$$\dot{y}_m \Big/ \frac{M_o T}{m \ell^2} = 3 \mu_m - 12 \frac{t}{T} \tag{34}$$

and

$$y_m \Big/ \frac{M_o T^2}{m \ell^2} = -\frac{3}{2} \mu_m + 3 \mu_m \left(\frac{t}{T}\right) - 6 \left(\frac{t}{T}\right)^2 \tag{35}$$

The motion of the beam terminates when the velocity $\dot{y}_m$ becomes zero, i.e., when

$$\dot{y}_m = \frac{3M_o}{m\ell^2}(\mu_m - 4)t \tag{30}$$

and

$$y_m = \frac{3M_o}{2m\ell^2}(\mu_m - 4)t^2 \tag{31}$$

The maximum displacement, expressed in terms of non-dimensional parameters, is

$$y_m \Big/ \frac{M_o T^2}{m\ell^2} = \frac{3}{2}(\mu_m - 4)\left(\frac{t}{T}\right)^2 \tag{32}$$

For $t > T$, the acceleration at the center becomes

$$\ddot{y}_m \Big/ \frac{M_o}{m\ell^2} = -12 \tag{33}$$

and the velocity and displacement are,

$$\dot{y}_m \Big/ \frac{M_o T}{m\ell^2} = 3\mu_m - 12\frac{t}{T} \tag{34}$$

and

$$y_m \Big/ \frac{M_o T^2}{m\ell^2} = -\frac{3}{2}\mu_m + 3\mu_m\left(\frac{t}{T}\right) - 6\left(\frac{t}{T}\right)^2 \tag{35}$$

The motion of the beam terminates when the velocity $\dot{y}_m$ becomes zero, i.e., when

$$\frac{t}{T} = \frac{1}{4} \mu_m \tag{36}$$

and the final permanent deformation is

$$y_m \Big/ \frac{M_o T^2}{m \ell^2} = \left(\frac{3}{8} \mu_m^2 - \frac{3}{2} \mu_m \right) \tag{37}$$

(c) $\mu_m > 36$ Since the applied load increases abruptly to $\mu_m > 36$, the motion of the beam also starts directly with the third phase, i.e. the beam deforms with three plastic hinges. The calculation of the motion of the beam, however is simplified by the fact that at the initial instant and also during the entire period between $t = 0$ and $t = T$, the inertia load g_2 is zero. Since the beam is stationary at the initial condition, the angular velocities $\dot{\theta}_0$ and $\dot{\theta}_1$ and hence $(\dot{\theta}_1 - \dot{\theta}_0)$ must be zero at $t = 0$. It can be seen from Equation (17) that g_2 must be zero at $t = 0$.

By setting $g_2 = 0$ in Equation (28) we obtain a relation between μ_m and ζ_h.

$$\mu_m = \frac{3}{2} \frac{(12 \zeta_h^2 + 4 \zeta_h - 1)}{(1 - 2\zeta_h) \zeta_h^2} \tag{38}$$

This relation determines the initial location of the plastic hinge at either side of the center when the load jumps abruptly to $\mu > 36$. A plot of ζ_h vs μ_m is shown in Figure 8.

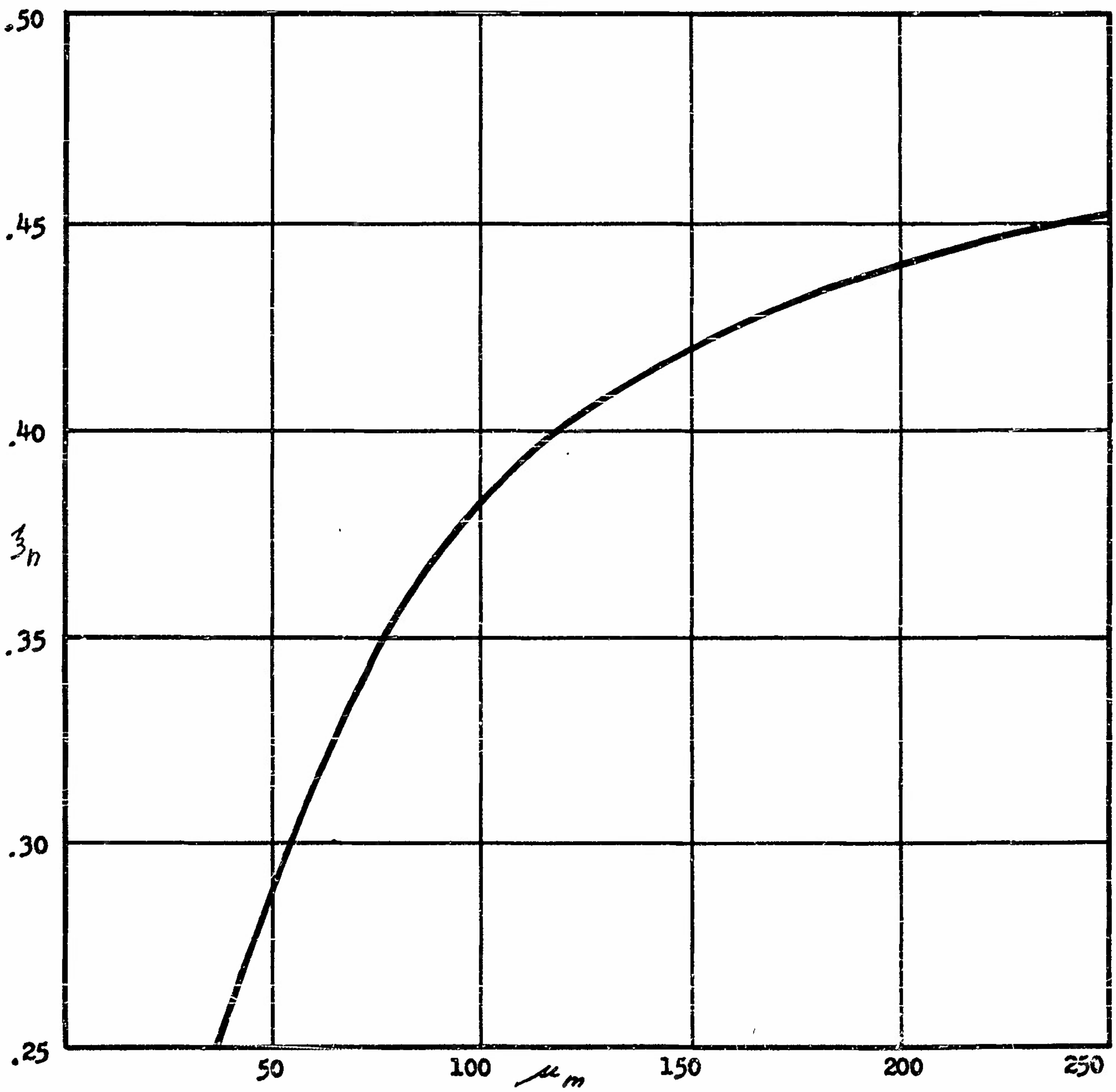

ζ_h vs. μ_m

Figure 8.

It can be seen that for higher impact load, the plastic hinge is closer to the center of the beam, and in the limiting case when μ_m approaches infinity, ξ_h approaches $\frac{1}{2}$. The range of ξ_h is thus,

$$1/4 < \xi_h < 1/2 \tag{38}$$

The acceleration at the center of the beam at the initial instant is

$$\ddot{y}_m = 1/m(g_0 + g_1) = \frac{6(4\xi_h^2 + 4\xi_h - 1)}{m(1-2\xi_h)^2 \xi_h^2} \; M_0/\ell^2 \tag{39}$$

For the rest of the period during which the constant load is applied the acceleration of the beam must retain the same constant value, and the hinge point remains at the same place. This is a sufficient condition, since with $\dot{x}_h$ vanishing, g_2 remains zero, and hence the acceleration obtained by Equation (39) must certainly satisfy the equilibrium conditions. An analysis is given in the appendix, to prove that this is a necessary condition.

The linear velocity and displacement of the beam can be readily evaluated by integration,

$$\dot{y}_m \Big/ \frac{M_0 T}{m \ell^2} = \frac{6(4\xi_h^2 + 4\xi_h - 1)}{(1-2\xi_h)^2 \; \xi_h^2} \; t/T \tag{40}$$

and

$$q_m \Big/ \frac{M_0 T^2}{m \ell^2} = \frac{3(4\zeta_n^2 + 4\zeta_n - 1)}{(1-2\zeta_n)^2 \zeta_n^2} \left(\frac{t}{T}\right)^2 \tag{41}$$

At $t = T$,

$$\dot{q}_m \Big/ \frac{M_0 T}{m \ell^2} = \frac{6(4\zeta_n^2 + 4\zeta_n - 1)}{(1-2\zeta_n)^2 \zeta_n^2} \tag{42}$$

$$q_m \Big/ \frac{M_0 T^2}{m \ell^2} = \frac{3(4\zeta_n^2 + 4\zeta_n - 1)}{(1-2\zeta_n)^2 \zeta_n^2} \tag{43}$$

The motion of the beam in the subsequent period, when the load P_m has been released, is again governed by the set of equations (25) to (28). The expressions for g_1 and g_2 are obtained by putting μ equal to zero

$$g_1 = -\frac{3(1 - 6\zeta_n + 12\zeta_n^2 + 56\zeta_n^3)}{2(1-2\zeta_n)^2 \zeta_n^3} \frac{M_0}{\ell^2} = F_1(\zeta_n) \frac{M_0}{\ell^2} \tag{44}$$

and

$$g_2 = -\frac{3(1 - 4\zeta_n - 12\zeta_n^2)}{(1-2\zeta_n)^2 \zeta_n^2} \frac{M_0}{\ell^2} = F_2(\zeta_n) \frac{M_0}{\ell^2} \tag{45}$$

By substituting Equations (44) and (45) into Equations (25) we obtain,

$$\frac{F_1(\xi_h)}{1-2\xi_h} = \frac{\dot{\xi}_h^{2}\, d/d\xi_h[F_2(\xi_h)] - F_2(\xi_h)\,\ddot{\xi}_h}{(\dot{\xi}_h)^2} \tag{46}$$

or, by rearranging, we obtain the following differential equation,

$$\ddot{\xi}_h = F(\xi_h)\,\dot{\xi}_h^2 \tag{47}$$

where

$$F(\xi_h) = -\frac{(1-2\xi_h)^2}{(1+2\xi_h)(1-6\xi_h)\xi_h} \tag{48}$$

The non-linear equation (47), however, can be solved in closed form as follows:

We see that

$$\frac{\ddot{\xi}_h}{(\dot{\xi}_h)^2} = -\frac{d}{dt}\frac{1}{\dot{\xi}_h} = -\dot{\xi}_h\frac{d}{d\xi_h}\left(\frac{1}{\dot{\xi}_h}\right) \tag{49}$$

and that by a transformation of variable,

$$z = 1/\dot{\xi}_h \tag{50}$$

we obtain, in place of Equation (47),

$$\frac{dz}{d\xi_h} + F(\xi_h)\,z = 0 \tag{51}$$

The initial value of z can be determined by observing from Equation (25) that at $t = T$,

$$\dot{\zeta}_h = -\frac{g_2}{2\int_0^T \frac{g_1\,dt}{1-2\zeta_h}} \tag{52}$$

Here g_2 is given by Equation (45) and g_1 by Equation (27), and the integral in Equation (52) becomes

$$\int_0^T \frac{g_1\,dt}{1-2\zeta_h} = \frac{3}{2}\,\frac{(16\zeta_h^3 + 12\zeta_h^2 - 1)\,T}{(1-2\zeta_h)^3\,\zeta_h^3}\;\frac{M_0}{\ell^2}$$

Thus the value of $\dot{\zeta}_h$ at $t = T$ is

$$\dot{\zeta}_h = -\frac{(1-6\zeta_h)(1-2\zeta_h)\zeta_h}{(1+2\zeta_h)(1-4\zeta_h)\,T} \tag{53}$$

Since, at $t = T$, $\zeta_h = \bar{\zeta}_h$, $\bar{\zeta}_h$ being the solution of Equation (38) for given value of μ_m the initial condition of z can be written at $\zeta_h = \bar{\zeta}_h$, as

$$z = \frac{1}{\dot{\zeta}_h} = -\frac{(1+2\bar{\zeta}_h)(1-4\bar{\zeta}_h)\,T}{(1-6\bar{\zeta}_h)(1-2\bar{\zeta}_h)\,\bar{\zeta}_h} \tag{54}$$

The solution of Equation (51) is

$$z = e^{-\int F(\xi_h)\,d\xi_h + C} = \frac{C_1 \xi_h}{(1+2\xi_h)(1-6\xi_h)^{\frac{1}{3}}} \tag{55}$$

in which the integrations constant C_1, determined by the initial condition, is

$$C_1 = -\frac{(1+2\bar{\xi}_h)^2(1-4\bar{\xi}_h)\,T}{(1-6\bar{\xi}_h)^{\frac{2}{3}}(1-2\bar{\xi}_h)\,\bar{\xi}_h^{\,2}} \tag{56}$$

Next we determine the time history of the hinge position ξ_h by solving the following differential equation,

$$\frac{d\xi_h}{dt} = \frac{1}{z} = \frac{(1+2\xi_h)(1-6\xi_h)^{\frac{1}{3}}}{C_1 \xi_h} \tag{57}$$

with the initial condition that at $t = T$, $\xi_h = \bar{\xi}_h$. We rewrite Equation (57) in the form,

$$dt = \frac{C_1 \xi_h\, d\xi_h}{(1+2\xi_h)(1-6\xi_h)^{\frac{1}{3}}} \tag{58}$$

and obtain the relation between t and ξ_h by direct integration. By introducing a transformation of variable,

$$\eta = (1-6\xi_h)^{\frac{1}{3}}$$
$$\bar{\eta} = (1-6\bar{\xi}_h)^{\frac{1}{3}} \tag{59}$$

we obtain

$$t = \int_{\bar{\eta}}^{\eta} - \frac{C_1}{4} \frac{(1-p^3)p}{(4-p^3)} dp + T$$

$$= -\frac{C_1}{4}\left[-\frac{1}{2\sqrt[3]{4}} \log \frac{4^{\frac{2}{3}}+4^{\frac{1}{3}}p+p^2}{(4^{\frac{1}{3}}-p)^2} + \frac{\sqrt{3}}{4^{\frac{1}{3}}} \tan^{-1} \frac{2p+4^{\frac{1}{3}}}{4^{\frac{1}{3}}\sqrt{3}} + \frac{p^2}{2}\right]_{\bar{\eta}}^{\eta} + T \qquad (60)$$

It should be observed from Equation (53) that since $\bar{\xi}_h$ lies within the range 1/4 to 1/2, $\dot{\xi}_h$ is always negative. This means, as we would expect, that the hinge point starts to move away from the center of the beam when the load has been released. It can also be seen from Equations (56) and (57) that $\dot{\xi}_h$ remains negative, and becomes zero when ξ_h reaches the value 1/6. This limiting condition, in fact, is the termination of the third phase of motion, when the difference in angular velocity $\dot{\theta}_1 - \dot{\theta}_0$ becomes zero, and hence when the plastic hinge at either side of the center disappears, it can be seen from Equation (22) that $\dot{\theta}_1 - \dot{\theta}_0$ is proportional to the ratio $q_2 / \dot{\xi}_h$. This ratio obtained from Equations (45) and (57) is,

$$\frac{q_2}{\dot{\xi}_h} = - \frac{3(1-6\xi_h)^{\frac{2}{3}} C_1 M_0}{(1-2\xi_h)^2 \xi_h \ell^2} \qquad (61)$$

and apparently, vanishes at $\xi_h = 1/6$.

It can be seen from Equation (60) that the instant T_1 at which the third phase of motion terminates is

$$T_1 = + \frac{c_1}{4}\left[-\frac{1}{2\sqrt[3]{4}} \log \frac{4^{\frac{2}{3}}+4^{\frac{1}{3}}\bar{\eta}+\bar{\eta}^2}{(4^{\frac{1}{3}}-\bar{\eta})^2} + \frac{\sqrt{3}}{4^{\frac{1}{3}}}\left(\tan \frac{2\bar{\eta}+4^{\frac{1}{3}}}{4^{\frac{1}{3}}\sqrt{3}} - \frac{\pi}{6}\right) + \frac{\bar{\eta}^2}{2}\right] + T \quad (62)$$

The acceleration at the center of the beam during this period is

$$\ddot{y}_m = -(q_0 + q_1 + q_2)/m$$

which by combination of Equations (26), (44) and (45) reduces to

$$\ddot{y}_m = -\frac{48}{(1-2\xi_h)^2}\frac{M_0}{m\ell^2} \quad (63)$$

The linear velocity and displacement at the center of the beam can, thus, be expressed as follows,

$$\dot{y}_m = (\dot{y}_m)_{t=T} + \int_T^t \ddot{y}_m \, dt \quad (64)$$

$$y_m = (y_m)_{t=T} + (\dot{y}_m)_{t=T}(t-T) + \int_T^t\int_T^t \ddot{y}_m \, dt\, dt \quad (65)$$

By making use of Equations (39), (42) and (43), we obtain, the following non-dimensional expressions,

$$\dot{y}_m \Big/ \frac{M_0 T}{m \ell^2} = \frac{6(4\bar{\xi}_h^2 + 4\bar{\xi}_h - 1)}{(1-2\bar{\xi}_h)^2 \bar{\xi}_h^2} + G \tag{66}$$

$$y_m \Big/ \frac{M_0 T^2}{m \ell^2} = \frac{6(4\bar{\xi}_h + 4\bar{\xi}_h - 1)}{(1-2\bar{\xi}_h)^2 \bar{\xi}_h^2}\left(\tau - \frac{1}{2}\right) + \int_1^{\tau} G\, d\tau \tag{67}$$

where

$$G = \frac{1}{\frac{M_0 T}{m \ell^2}} \int_T^t \ddot{y}_m \, dt \tag{68}$$

and

$$\tau = t/T \tag{69}$$

The integral G, can be evaluated in closed form. We obtain, by substituting Equation (63) into (68),

$$G = -\frac{48}{T}\int_T^t \frac{1}{(1-2\xi_h)^2}\, dt \tag{70}$$

which by introducing Equation (58), is reduced to

$$G = -\frac{48}{T}\int_{\bar{\xi}_h}^{\xi_h} \frac{\xi_h \, d\xi_h}{(1+2\xi_h)(1-6\xi_h)^{\frac{1}{3}}(1-2\xi_h)^2}$$

This integral, when evaluated by the use of the transformation of variable,

$$\eta = (1-6\xi_n)^{\frac{1}{3}}, \quad \bar{\eta} = (1-6\bar{\xi}_n)^{\frac{1}{3}}$$

becomes

$$G = -\frac{9C_1}{T}\left[\frac{1}{6\sqrt[3]{4}}\log\frac{4^{\frac{2}{3}}+4^{\frac{1}{3}}\eta+\eta^2}{(4^{\frac{1}{3}}-\eta)^2} - \frac{1}{4^{\frac{1}{3}}\sqrt{3}}\tan^{-1}\frac{2\eta+4^{\frac{1}{3}}}{4^{\frac{1}{3}}\sqrt{3}} - \left(\frac{\eta^2}{2+\eta^3}\right)\right]_{\bar{\eta}}^{\eta} \tag{71}$$

it is seen that at $t = T_1$, $\eta = 0$, and

$$G(T_1) = \frac{9C_1}{T}\left[\frac{1}{6\sqrt[3]{4}}\log\frac{4^{\frac{2}{3}}+4^{\frac{1}{3}}\bar{\eta}+\bar{\eta}^2}{(4^{\frac{1}{3}}-\bar{\eta})^2} - \frac{1}{4^{\frac{1}{3}}\sqrt{3}}\left(\tan^{-1}\frac{2\bar{\eta}+4^{\frac{1}{3}}}{4^{\frac{1}{3}}\sqrt{3}} - \frac{\pi}{6}\right) - \frac{\bar{\eta}^2}{2+\bar{\eta}^3}\right] \tag{72}$$

Having determined the G-function, we can evaluate the integral $\int_1^{\tau} G\,d\tau$ in Equation (67) by means of numerical integration.

After the plastic hinge at either side of the mid-point has been removed, the acceleration of the beam is again governed by Equation (6) except that in this case μ is equal to zero, thus

$$\ddot{y}_m = -\frac{12\,M_0}{m\ell^2} \tag{73}$$

and

$$\dot{y}_m = \dot{y}_{t=T_1} - \frac{12\,M_0}{m\ell^2}(t-T_1) \tag{74}$$

The hinge action at the center of the beam ceases when the linear velocity becomes zero. It can be seen from Equation (74) that at this instant

$$t - T_1 = \dot{y}_{m_{t=T_1}} \Big/ \frac{12 M_0}{m l^2} \tag{75}$$

and the final displacement, which is the permanent set of the beam due to impact, is

$$y_{m_p} = y_{m_{t=T_1}} + \frac{1}{2}\left(\dot{y}_{m_{t=T_1}}\right)^2 \Big/ \frac{12 M_0}{m l^2} \tag{76}$$

In non-dimensional form, the expression becomes

$$y_{m_p} \Big/ \frac{M_0 T^2}{m l^2} = \frac{6(4\bar{\xi}_h^2 + 4\bar{\xi}_h - 1)}{(1-2\bar{\xi}_h)^2 \bar{\xi}_h^2}\left(\tau_1 - \frac{1}{2}\right) + \int_1^{\tau_1} G\, d\tau$$
$$+ \frac{1}{24}\left[\frac{6(4\bar{\xi}_h^2 + 4\bar{\xi}_h - 1)}{(1-2\bar{\xi}_h)^2 \bar{\xi}_h^2} + G(\tau_1)\right]^2 \tag{77}$$

IV Results and Discussion

The final permanent deformation of the beam, $y_{m_p} \big/ \frac{M_0 T^2}{m l^2}$, can be determined either by Equation (37) for $4 < \mu_m < 36$ or by Equation (77) for $\mu_m > 36$. Figure 10 shows the variation of this parameter as a function of the impact force parameter μ_m. In the calculation of this final result, the values of $\bar{\xi}_h$, τ_1, $G(\tau_1)$, $\int_1^{\tau_1} G\, d\tau$ for various values of μ_m are required.

A plot of $\bar{\zeta}_h$ vs. μ_m has been given in Figure 8, while the relations between τ_1 and $G(\tau_1)$ vs. $\bar{\zeta}_h$, obtained respectively by Equations (62) and (72) are plotted in Figure (9). The integral $\int_1^{\tau_1} G\,d\tau$, obtained by a numerical method, is also plotted in the same figure.

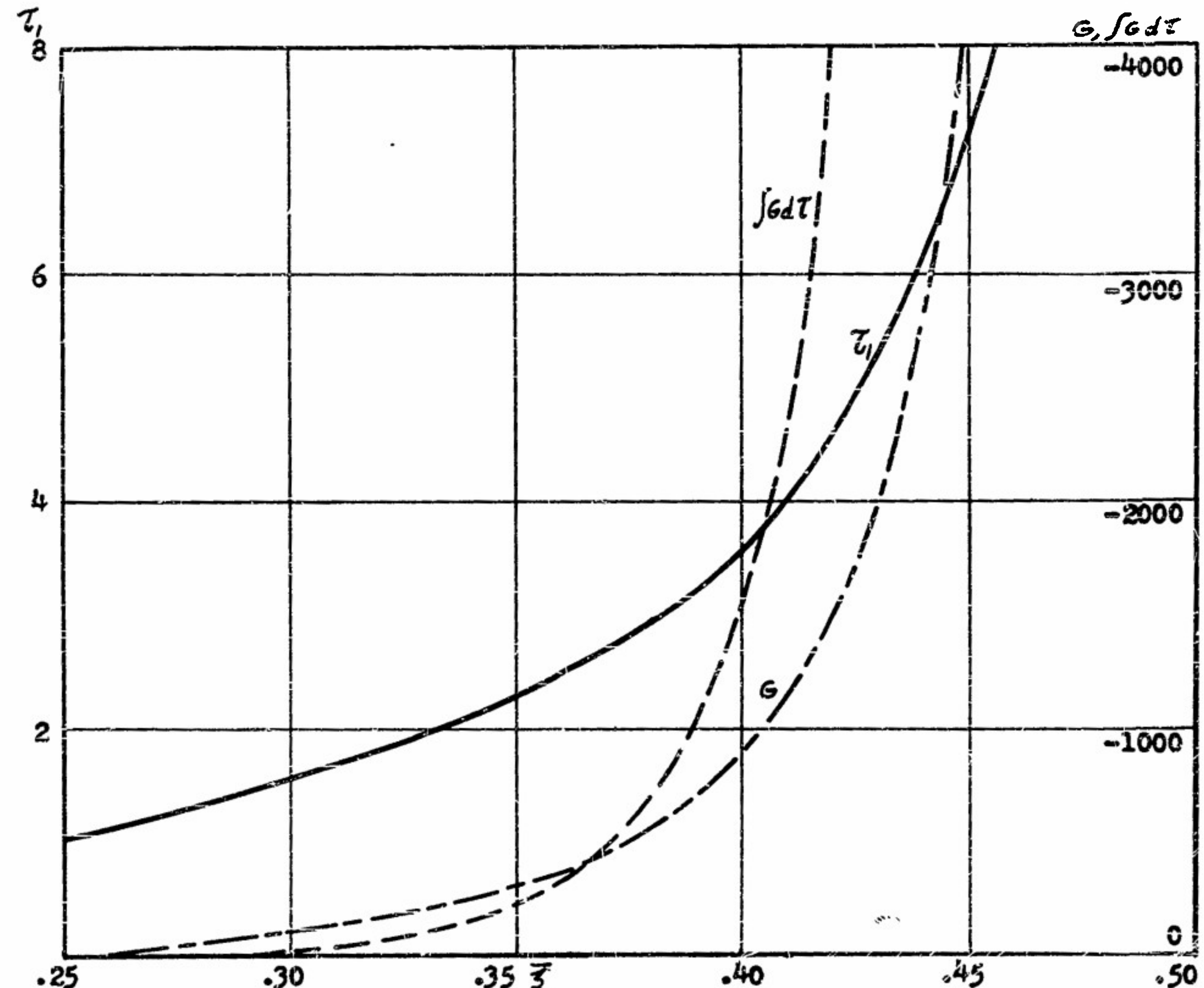

Figure 9.

Figure (11) shows the variation of the displacement parameter $y/\frac{M_0 T^2}{m l^2}$ with respect to time. It can be seen that in all cases the increase in displacement after the end of impact, constitutes the major part of the

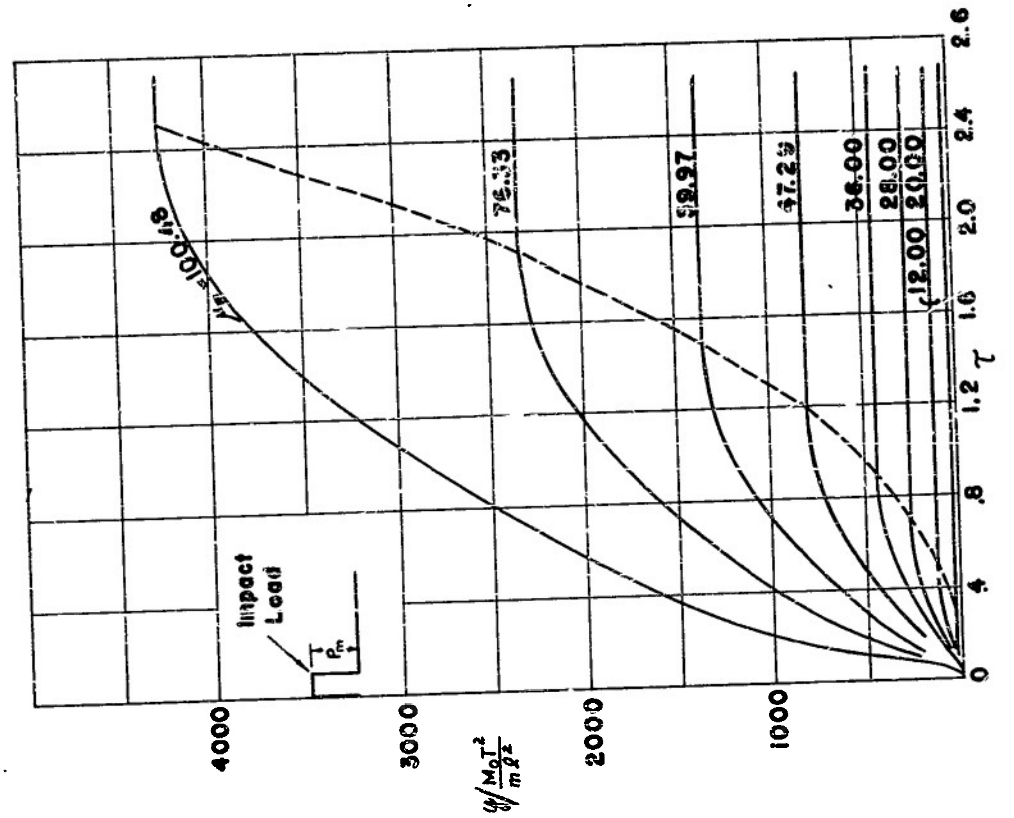
Impact Load
$\mu_m = 100.48$
76.33
59.97
47.23
36.00
28.00
20.00
12.00
0
.4
.8
1.2
1.6
2.0
2.4
2.6
τ
4000
3000
2000
1000
$\psi / \frac{M_o T^2}{m \ell^2}$

Fig. (11)

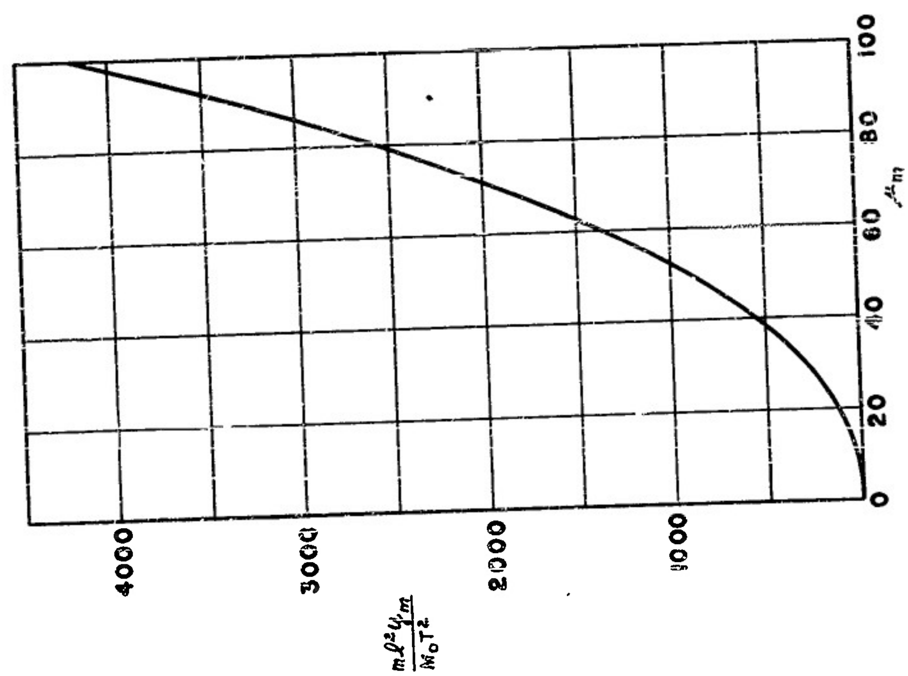
0
20
40
60
80
100
μ_m
4000
3000
2000
1000
$\frac{m \ell^2 \psi_m}{M_o T^2}$

Fig. (10)

permanent deformation of the beam.

It should be stated that a criterion, similar to that given in Reference 1, can be drawn for the conditions of validity of the present method of analysis. The criterion is based on the requirement that the plastic work done at the center hinge be large compared with the maximum elastic energy which could be stored in the beam in bending when the whole beam is subject to the limit moment M_o. This criterion is:

$$M_o \theta_1 \gg \frac{M_o^2 \ell}{2EI} \tag{78}$$

This can be rewritten into a more convenient form;

$$\theta_1 \Big/ \frac{M_o T^2}{m \ell^3} \gg 1.25 \left(\frac{T_N}{T} \right)^2 \tag{79}$$

where T_N is the fundamental period of vibration of the simply supported elastic beam. Since the values of θ_1 have not been evaluated; and since is always larger than $y_m / \frac{\ell}{2}$, the above criterion is now replaced by

$$y_m \Big/ \frac{M_o T^2}{m \ell^2} \gg 2.5 \left(\frac{T_N}{T} \right)^2 \tag{80}$$

This relation gives the lower limit on the duration of impact above which the present analysis can be expected to give satisfactory results.

References

1. Lee, E. H. and Symonds, P. S. "Large Plastic Deformations of Beams Under Transverse Impact" Brown University Technical Report B11-3/28, Contract N7onr-35810, NR-360-364. Sept. 1951.

Appendix A

Proof of Necessity of Stationary Hinges During Period of Constant Impact Load

It has been stated in Section III of the main body of the report that during the period when a constant impact load (with $\mu > 36$) is applied, the second hinge point remains at the same location. A proof of this statement is given in the present appendix.

During this period, the motion of the beam is determined by equations (25) to (28). Since, for prescribed amplitude of impact, g_1 and g_2 are functions of ξ_h only, equation (25) can be rewritten as

$$\frac{g_1(\xi_h)}{1-2\xi_h} = -\frac{\dot{\xi}_h^2 \frac{d}{d\xi_h} g_2(\xi_h) - g_2(\xi_h)\ddot{\xi}_h}{2\dot{\xi}_h^2} \qquad (A.1)$$

or, by rearranging terms,

$$\ddot{\xi}_h = \frac{\frac{2g_1(\xi_h)}{1-2\xi_h} + \frac{d}{d\xi_h} g_2(\xi_h)}{g_2(\xi_h)} \dot{\xi}_h^2 \qquad (A.2)$$

By substituting equations (27) and (28) into equation (A.2) and simplifying, we obtain the following differential equation

$$\ddot{\xi}_h = \dot{\xi}_h^2 / H(\xi_h) \qquad (A.3)$$

where

$$H(\xi_h) = \frac{-2\mu_m(1-2\xi_h)\xi_h^3 - 3(1+2\xi_h)(1-6\xi_h)\xi_h}{8\mu\xi_h^3 + 3(1-2\xi_h)^2} \qquad (A.4)$$

It is obvious that at $t = 0$

$$\xi_h = \xi_{h_0}$$

where ξ_{h_0} is the solution of equation (38). It will be shown here that at the initial instant $\dot{\xi}_h$ and all the higher derivatives are zero.

It can be seen from Equation (17) that $\dot{\xi}_h$ can be written as

$$\dot{\xi}_h(0) = -\left(\frac{q_2}{\dot{\theta}_1 - \dot{\theta}_0}\ \frac{\ell^2}{M_0}\right)_{t=0} \qquad (A.5)$$

This is of the indeterminate form since, at the initial instant both g_2 and $(\dot{\theta}_1 - \dot{\theta}_0)$ are zero. However by applying L'Hopital's rule, we can write,

$$\dot{\xi}_h(0) = -\left(\frac{\frac{dq_2}{dt}}{\ddot{\theta}_1 - \ddot{\theta}_0}\ \frac{\ell^2}{M_0}\right)_{t=0} \qquad (A.6)$$

which, by introducing Equation (16), becomes,

$$\dot{\xi}_h(0) = -\left(\frac{\frac{dq_2}{dt}}{\frac{2q_1}{1-2\xi_h}}\right)_{t=0} = -\left(\frac{\dot{\xi}_h \frac{dq_2}{d\xi_h}(1-2\xi_h)}{2q_1}\right)_{t=0} \qquad (A.7)$$

We see that this is true either when $\dot{\xi}_h(0)$ vanishes or when $\left(-\frac{dq_2}{d\xi_h}(1-2\xi_h)/2q_1\right)_{t=0}$ is equal to unity.

By introducing Equations (27) and (28), we obtain

$$\left(-\frac{dq_2}{d\xi_h}(1-2\xi_h)/2q_1\right)_{t=0} = \frac{4\mu_m(1-2\xi_h)\xi_h^3+3(-2+12\xi_h-24\xi_h^2-48\xi_h^3)}{12\mu_m(1-2\xi_h)\xi_h^3-(1-6\xi_h+12\xi_h^2+56\xi_h^3)} \qquad (A.8)$$

and by substituting Equation (38) for μ_m, we have

$$\left(-\frac{dq_2}{d\xi_h}(1-2\xi_h)/2q_1\right)_{t=0} = \frac{2(1-5\xi_h+8\xi_h^2+12\xi_h^3)}{1-12\xi_h^2-16\xi_h^3} \qquad (A.9)$$

It can be shown that this quantity is always negative for values of ξ_h ranging from 1/4 to 1/2. Thus at the initial instant, $\dot{\xi}_h$ must be zero.

We see from the differential equation (A.3) that at the initial instant, $\ddot{\xi}_h$ is again indeterminate. However, by writing,

$$\ddot{\xi}_h(0) = \left(\frac{\frac{d}{dt}(\dot{\xi}_h)^2}{\frac{d}{dt}H(\xi_h)}\right)_{t=0} = \left(\frac{2\ddot{\xi}_h}{\frac{d}{d\xi}H(\xi_h)}\right)_{t=0} \qquad (A.5)$$

Here again since $\frac{1}{2}\frac{d}{d\xi}H(\xi_h)$ is not identically equal to unity, $\ddot{\xi}_h(0)$ must be zero. By differentiating Equation (A.3), we obtain an expression for $\dddot{\xi}_h$. We find in the same way, that $\dddot{\xi}(0)$ and also all the higher derivatives are zero. Thus, during the period $0 < t < T$, the hinge remains stationary at station ξ_{h_0}.

DISTRIBUTION LIST

Technical Reports

Contract N5ori-07833 Project NR 064-259

Chief of Naval Research
Department of the Navy
Washington 25, D.C.
Attn: Code 438 (2)

Commanding Officer
Office of Naval Research
Branch Office
495 Summer Street
Boston 10, Massachusetts (2)

Office of Naval Research
Branch Office
495 Summer Street
Boston 10, Massachusetts
Attn: Dr. H.R. Seiwell (1)

Chief of Bureau of Aeronautics
Navy Department
Washington 25, D.C.
Attn: TD-41, Technical Library (1)
: DE-22, C. W. Hurley (2)

Chief of Bureau of Ordnance
Navy Department
Washington 25, D.C.
Attn: Ad-3, Technical Library (1)
: Re9a (1)

Chief of Bureau of Ships
Navy Department
Washington 25, D.C.
Attn: Director of Research (1)
: Code 442 (1)

Chief of Bureau of Yards and Docks
Navy Department
Washington 25, D.C.
Attn: Research Division (2)

Librarian
U.S. Naval Postgraduate School
Monterey, California (1)

Naval Air Experimental Station
Naval Air Material Center
Naval Base
Philadelphia 12, Pa.
Attn: Head, Aeronautical Materials Laboratory (1)

Naval Ordnance Laboratory
Naval Gun Factory
Washington 25, D.C.
Attn: Dr. D.E. Marlowe (1)

Superintendent
Naval Gun Factory
Washington 25, D.C. (1)

Naval Ordnance Laboratory
White Oak, Maryland
RFD 1, Silver Spring, Maryland
Attn: Dr. C.A. Truesdell (1)

Naval Ordnance Test Station
Inyokern, California
Attn: Scientific Officer (1)

Director
David Taylor Model Basin
Washington 7, D.C.
Attn: Structural Mechanics Division (2)

Director
Naval Engineering Experiment Station
Annapolis, Maryland (1)

Director
Materials Laboratory
New York Naval Shipyard
Brooklyn 1, New York (1)

Chief of Staff
Department of the Army
The Pentagon
Washington 25, D.C.
Attn: Director of Research and Development (1)

Contract N5ori-07833 Project NR 064-259

Office of Chief of Ordnance
Research and Development Service
Department of the Army
The Pentagon
Washington 25, D.C.
Attn: ORDTB (1)

Commanding Officer
Watertown Arsenal
Watertown, Massachusetts
Attn: Laboratory Division (1)

Commanding Officer
Frankford Arsenal
Philadelphia, Pa.
Attn: Laboratory Division (1)

Commanding Officer
Squier Signal Laboratory
Fort Monmouth, New Jersey
Attn: Components and Materials Branch (1)

Commanding General
U.S. Air Forces
The Pentagon
Washington 25, D.C.
Attn: Research and Development Division (1)

Commanding General
Air Materiel Command
Wright-Patterson Air Force Base
Dayton, Ohio
Attn: E.H. Schwartz - MCREXA-8 (3)

Director
National Bureau of Standards
Washington, D. C.
Attn: Dr. W.H. Ramberg (1)

U.S. Coast Guard
1300 E Street, NW
Washington, D.C.
Attn: Chief, Testing and Development Division (1)

Forest Products Laboratory
Madison, Wisconsin
Attn: L.J. Markwardt (1)

National Advisory Committee for Aeronautics
1724 F Street, NW
Washington, D.C.
Attn: Materials Research Coordination Group (2)

National Advisory Committee for Aeronautics
Langley Field, Virginia
Attn: Mr. E. Lundquist (1)
: Dr. S. B. Batdorf (1)

National Advisory Committee for Aeronautics
Cleveland Municipal Airport
Cleveland, Ohio
Attn: J.H. Collins, Jr. (1)

U. S. Maritime Commission
Technical Bureau
Washington, D. C.
Attn: Mr. Wanless (1)

Research and Development Board
Pentagon Building
Washington, D. C.
Attn: Library 3D641 (1)

Dr. S. P. Timoshenko
School of Engineering
Stanford University
Stanford, California (1)

Dr. D. C. Drucker
Graduate Division of Applied Math.
Brown University
Providence, Rhode Island (1)

Dr. F. A. Biberstein, Jr.
Catholic University of America
Washington, D. C. (1)

Dr. J. E. Dorn
University of California
Berkeley, California (1)

Dr. T. J. Dolan
University of Illinois
Urbana, Illinois (1)

Professor R. L. Bisplinghoff
Massachusetts Institute of Technology
Cambridge 39, Massachusetts (15)

Contract N5ori-07833 Project NR 064-259

Dr. N. J. Hoff
Department of Aeronautical Engineering
and Applied Mechanics
Polytechnic Institute of Brooklyn
99 Livingston Street
Brooklyn, New York (1)

Dr. N. M. Newmark
Department of Civil Engineering
University of Illinois
Urbana, Illinois (1)

Dr. J. N. Goodier
School of Engineering
Stanford University
Stanford, California (1)

Professor F. K. Teichmann
Department of Aeronautical Engineering
New York University
University Heights, Bronx
New York City, New York (1)

Professor L. S. Jacobsen
Stanford University
Stanford, California (1)

Professor Jesse Ormondroyd
University of Michigan
Ann Arbor, Michigan (1)

Dr. W. H. Hoppmann
Department of Applied Mechanics
Johns Hopkins University
Baltimore, Maryland (1)

Professor W. K. Krefeld
College of Engineering
Columbia University
New York, New York (1)

Professor R. M. Hermes
University of Santa Clara
Santa Clara, California (1)

Professor B. J. Lazan
Syracuse University
Syracuse, New York (1)

Dr. J. M. Lessells
Lessells and Associates
916 Commonwealth Avenue
Boston 15, Massachusetts (1)

Dean L. M. K. Boelter
University of California
Los Angeles, California (1)

Professor P. Lieber
Polytechnic Institute of Brooklyn
99 Livingston Street
Brooklyn 2, New York (1)

Commanding Officer
Office of Naval Research
Branch Office
346 Broadway
New York 13, N. Y. (1)

Commanding Officer
Office of Naval Research
Branch Office
844 N. Rush Street
Chicago 11, Illinois (1)

Commanding Officer
Office of Naval Research
Branch Office
1000 Geary Street
San Francisco 9, Calif. (1)

Commanding Officer
Office of Naval Research
Branch Office
1030 Green Street
Pasadena, California (1)

Contract Administrator, SE Area
Office of Naval Research
Department of Navy
Washington 25, D. C.
Attn: Mr. R. F. Lynch (1)

Director, Naval Research Laboratory
Washington 20, D. C.
Attn: Technical Information Officer (9)
Technical Library (1)
Mechanics Division (2)

Dr. A. C. Eringen
Illinois Institute of Technology
Chicago, Illinois (1)

Dr. M. Hetenyi
Northwestern University
Evanston, Illinois (1)

Contract N5ori-07833

Project NR 064-259

Officer in Charge
Office of Naval Research
Branch Office
Navy #100
Fleet Post Office
New York, New York (5)

Dr. C. B. Smith
College of Arts and Sciences
Department of Mathematics
Walker Hall
University of Florida
Gainesville, Florida (1)